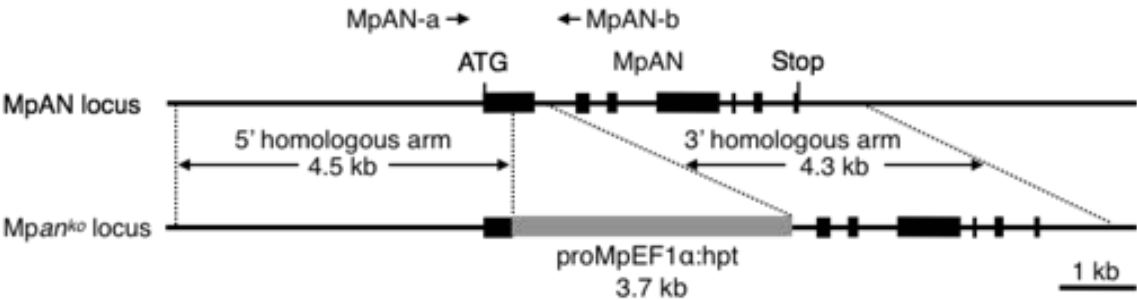


**Fig. S1. Expression pattern of MpAN gene.** (A, B) Expression levels (A) and expression profiles (B) of MpAN gene in various organs were extracted and visualized from the published RNA-seq data sets in Bowman et al., 2017 and the genome database for *M.polymorpha*, MarpolBase. (C) Expression levels of MpAN gene during gemmae, gemmalings, and developing antheridiophores and archegoniophores were analyzed by using RT-PCR. Expression levels of MpEF1 $\alpha$  were also indicated as a control. Total RNAs were extracted from gemmae indicated as G0, genmalings cultured for 1, 3, and 5 days indicated as G1, G3, and G5, and developing archegoniophores and antheridiophores indicated as F and M, respectively. (D, E) Expression pattern of *pMpAN:Citrine-NLS* (D) and *pMpAN:GUS-10* (E) in thallus of T1 transgenic plants were visualized. Citrine signals are shown in green and autofluorescence in red (D). (F, G, H, I, J, K, L) Expression pattern of *pMpAN:GUS-10* (male) (F, G, J, K) and *pMpAN:GUS-4* (female) (H, I, L) in reproductive organs were visualized. The early developmental stage of antheridiophores (F) and archegoniophores (H). Antheridial receptacle (G) and archegonial receptacle (I). Free-hand vertical section views of antheridial receptacle (J). Antheridium (K) and archegonium (L). Embryo of *pMpAN:GUS-4* (female) with *pMpAN:GUS-10* (male) (M). Bars, 100  $\mu$ m (E, D), 1 mm (F-I), 200  $\mu$ m (J), 100  $\mu$ m (K), 50  $\mu$ m (L, M).

A



B

AA	M G K G V T M P P E A S	S G R	
Tak-1	ATGGGCAAGGGCGTCACGATGCTCTCCGAGGCATCG	TCAGGGA	43
Mpan-4 <sup>ge</sup>	ATGGGCAAGGGCGTCACGATGCCTCCGAGGCATCGTAAACCCCATCCACCTC	CAGGGA	60
Mpan-9 <sup>ge</sup>	ATGGGCAAGGGCGTCACGATGCCTCCCGA		29

AA	V D G G R V A E R N P G S R Q I G K M R		
Tak-1	GGGTGGATGGGGGTAGGGTAGCGGAGAGAAATCCTGGTTCGCGGCAAAATGGAAAGATGC		103
Mpan-4 <sup>ge</sup>	GGGTGGATGGGGGTAGGGTAGCGGAGAGAAATCCTGGTTCGCGGCAAAATGGAAAGATGC		120
Mpan-9 <sup>ge</sup>			29

AA	S D G T V R K S K G Y E P L S M G L P L		
Tak-1	GGAGCGACGGGACTGTGAGGAAGTCAAAAGGTTACGAACCGCTCAGCATGGGATTACCTC		163
Mpan-4 <sup>ge</sup>	GGAGCGACGGGACTGTGAGGAAGTCAAAAGGTTACGAACCGCTCAGCATGGGATTACCTC		180
Mpan-9 <sup>ge</sup>			29

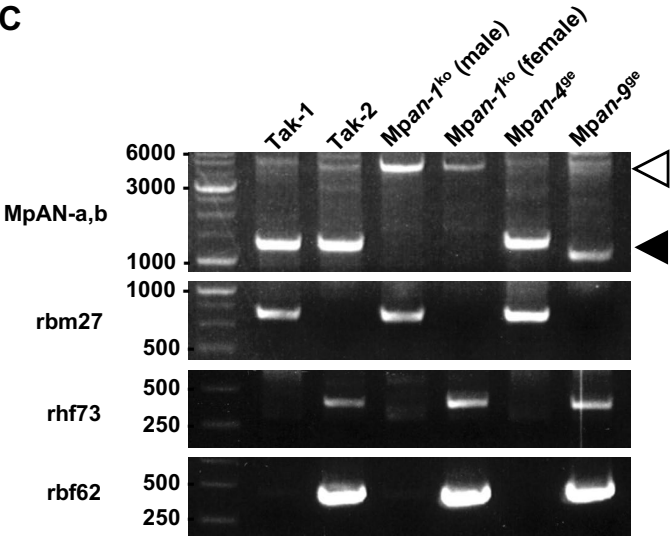
  

AA	V V A L N C M D D C R A E A E A L E G V		
Tak-1	TGGTCGTGGCTCTGAATTGCATGGACGATTGTCGTGCCGAAGCCGAGGCTTTGGAAGGAG		223
Mpan-4 <sup>ge</sup>	TGGTCGTGGCTCTGAATTGCATGGACGATTGTCGTGCCGAAGCCGAGGCTTTGGAAGGAG		240
Mpan-9 <sup>ge</sup>			29

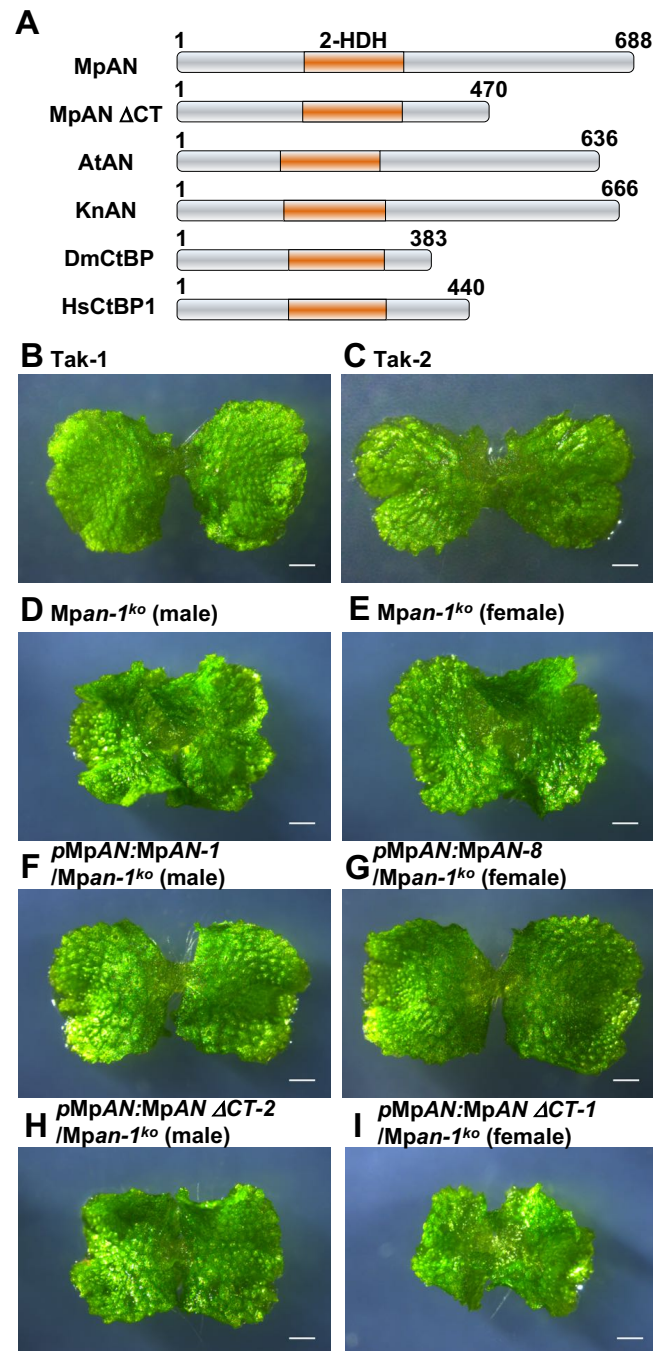
  

AA	A V V E H V G L A Q V G E G K I E A A V		
Tak-1	TGGCTGTAGTTGAGCATGTGGGTCTCGCCAGGTTGGAGAAGGAAAGATCGAAGCGGCCG		283
Mpan-4 <sup>ge</sup>	TGGCTGTAGTTGAGCATGTGGGTCTCGCCAGGTTGGAGAAGGAAAGATCGAAGCGGCCG		300
Mpan-9 <sup>ge</sup>	GGTCTCGCCAGGTTGGAGAAGGAAAGATCGAAGCGGCCG		69

C



**Fig. S2. Construction of *Mpan* knock-out (*Mpan*<sup>ko</sup>) and *Mpan* genome-edited (*Mpan*<sup>ge</sup>) lines.** (A) Genomic structures in the wild-type (Tak-1) and *Mpan* knock-out (*Mpan*-1<sup>ko</sup>) lines. MpAN exons are indicated by black boxes. The hygromycin phosphotransferase gene (*hpt*) cassette is indicated by the gray box. (B) Genomic sequences in the Tak-1 and genome-edited lines. The amino acid (AA) sequence encoded by MpAN is shown at top. The Tak-1 sequence is shown together with the PAM sequence (red) and the target sequence (blue). The genome-edited lines *Mpan*-4<sup>ge</sup> and *Mpan*-9<sup>ge</sup> have a 17 bp insertion and 214 bp deletion, respectively (orange). (C) Genotyping of the wild-type, *Mpan* knock-out, and genome-edited lines. The positions of the primers used to confirm knock-out and genome editing of MpAN are shown in *a*. Black and white arrowheads indicate the predicted sizes of the PCR products from the wild-type and knock-out *Mpan* genomes, respectively. The Y-chromosome-linked DNA marker *rbm27* and the X-chromosome-linked DNA markers *rhf73* and *rbf62* were used for sexual genotyping.



**Fig. S3. Morphology of *pMpAN:MpAN  $\Delta$ CT/ Mpan-1<sup>ko</sup>* plants.** (A) Schematic representation of plant ANs and animal CtBPs. MpAN  $\Delta$ CT is deleted for the plant specific C-terminal region. (B) Genotyping of the complementation lines. (B-I) 10-day-old gemmalings of Tak-1 (B), Tak-2 (C), *Mpan-1<sup>ko</sup>* (male) (D), *Mpan-1<sup>ko</sup>* (female) (E), *pMpAN:MpAN-1/Mpan-1<sup>ko</sup>* (male) (F), *pMpAN:MpAN-8/Mpan-1<sup>ko</sup>* (female) (G), *pMpAN:MpAN  $\Delta$ CT-2/Mpan-1<sup>ko</sup>* (male) (H), and *pMpAN:MpAN  $\Delta$ CT-1/Mpan-1<sup>ko</sup>* (female) (I). Bars, 1 mm.



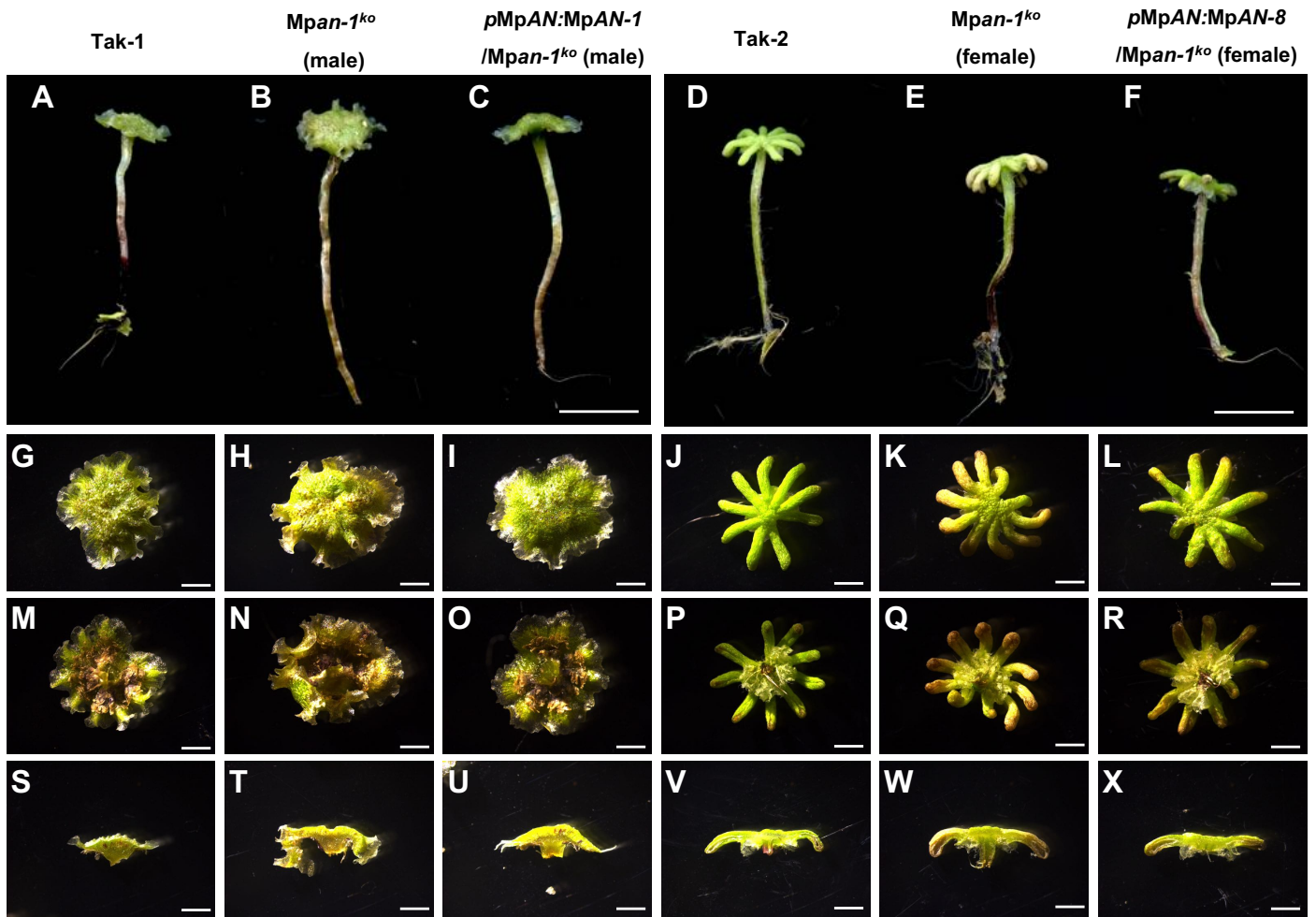
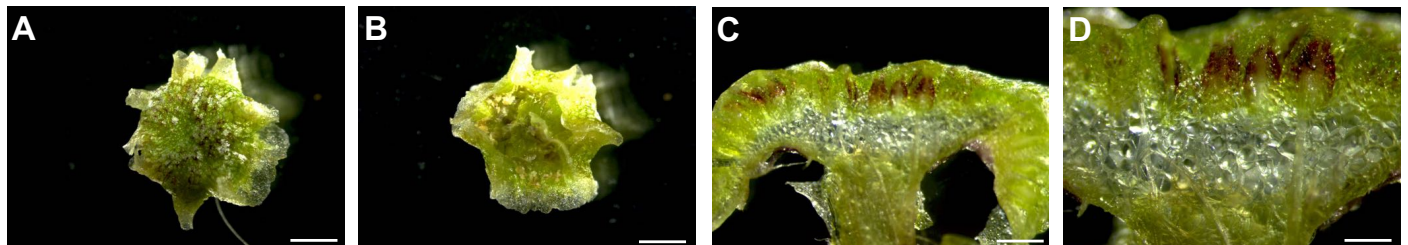
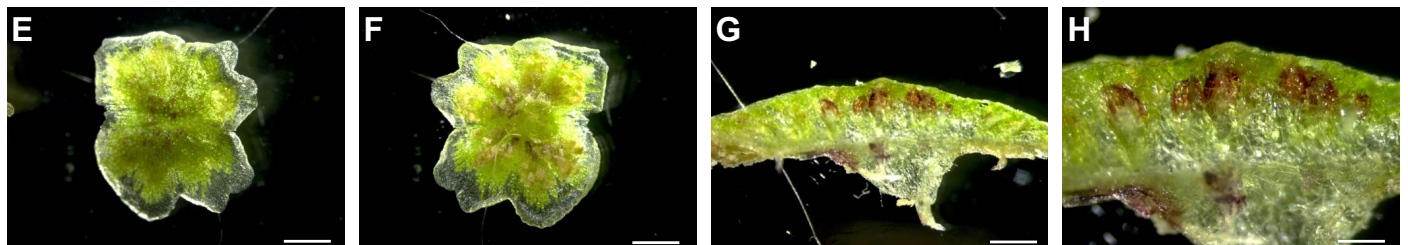


**Fig. S4. Morphology of antheridiophores and archegoniophores of *Mpan* mutants.** (A–F) Side views of antheridiophores of Tak-1 (A), *Mpan-1<sup>ko</sup>* (male) (B), and *pMpAN:MpAN-1/Mpan-1<sup>ko</sup>* (male) (C) and archegoniophores of Tak-2 (D), *Mpan-1<sup>ko</sup>* (female) (E), and *pMpAN:MpAN-8/Mpan-1<sup>ko</sup>* (female) (F). Bars, 1 cm. (G–R) Dorsal (G–L) and ventral (M–R) side views of antheridiophores of Tak-1 (G,M), *Mpan-1<sup>ko</sup>* (male) (H,N), and *pMpAN:MpAN-1/Mpan-1<sup>ko</sup>* (male) (I,O) and archegoniophores of Tak-2 (J,P), *Mpan-1<sup>ko</sup>* (female) (K,Q), and *pMpAN:MpAN-8/Mpan-1<sup>ko</sup>* (female) (L,R). Bars, 3 mm. (S–X) Free-hand vertical section views of antheridiophores of Tak-1 (S), *Mpan-1<sup>ko</sup>* (male) (T), and *pMpAN:MpAN-1/Mpan-1<sup>ko</sup>* (male) (U) and archegoniophores of Tak-2 (V), *Mpan-1<sup>ko</sup>* (female) (W), and *pMpAN:MpAN-8/Mpan-1<sup>ko</sup>* (female) (X). Bars, 3 mm.

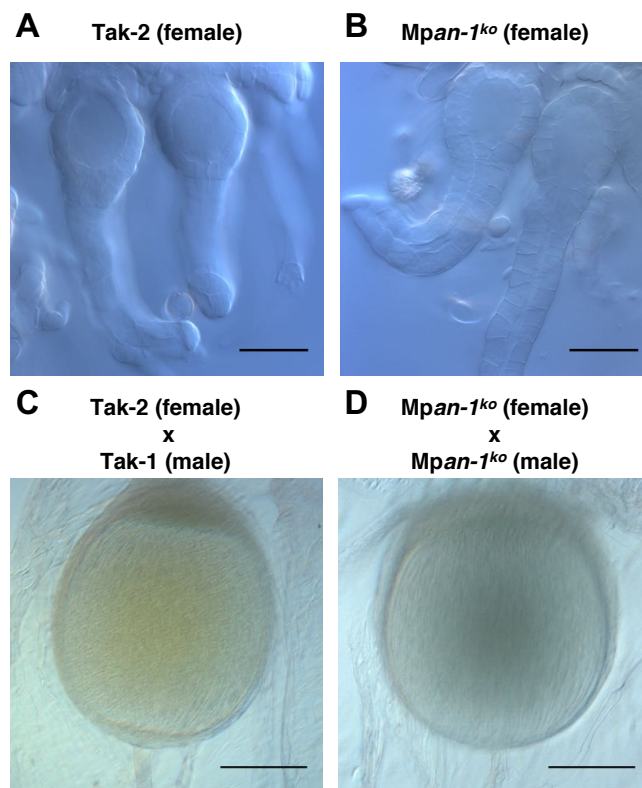
***Mpan-1<sup>ko</sup>* (male)**



***pMpAN:MpAN-1/Mpan-1<sup>ko</sup>* (male)**

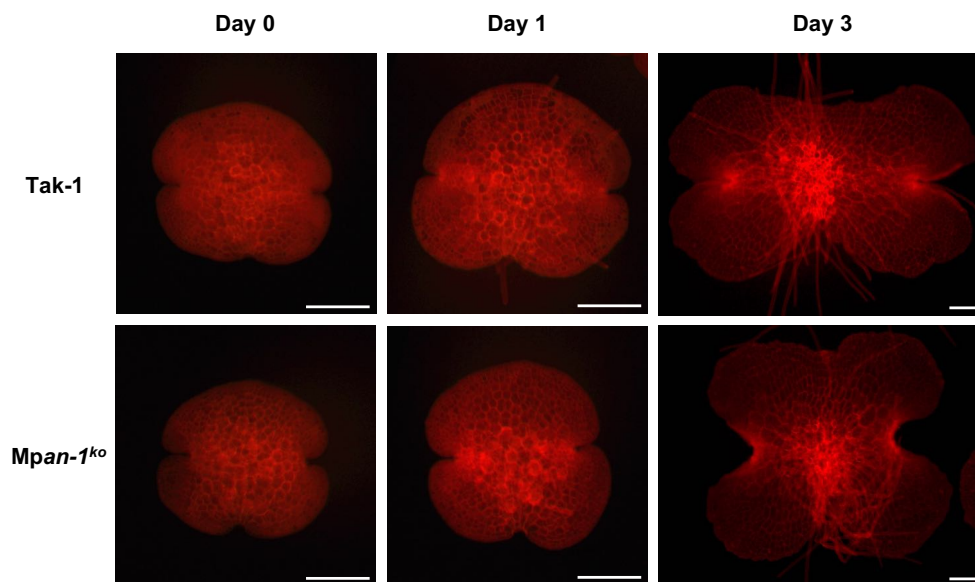


**Fig. S5. Morphology of antheridiophores of *Mpan* mutants.** (A–H) Antheridiophores of *Mpan-1<sup>ko</sup>* (male) (A–D) and *pMpAN:MpAN-1/Mpan-1<sup>ko</sup>* (male) (E–H). Dorsal (A, E), ventral (B, F), and free-hand vertical section (C, D, G, H) views. Bars, 3 mm (A, B, E, F), 0.8 mm (C, G), and 0.4 mm (D, H).

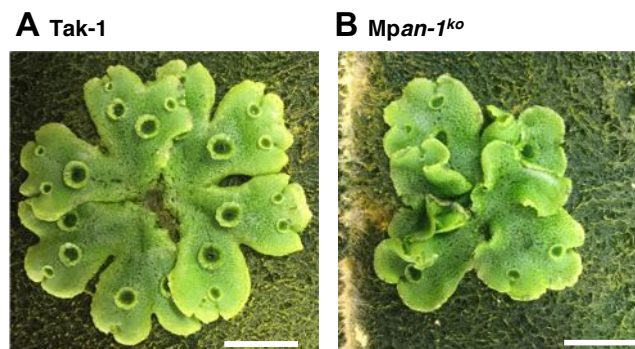


**Fig. S6. Morphology of archegonians and sporophytes of *Mpan* mutants.** Archegonians of Tak-2 (A) and *Mpan-1<sup>ko</sup>* (female) (B). Sporophytes of Tak-2 with Tak-1 (C) and of *Mpan-1<sup>ko</sup>* (female) with *Mpan-1<sup>ko</sup>* (male) (D). Bars, 50 μm (A, B), and 200 μm (C, D).

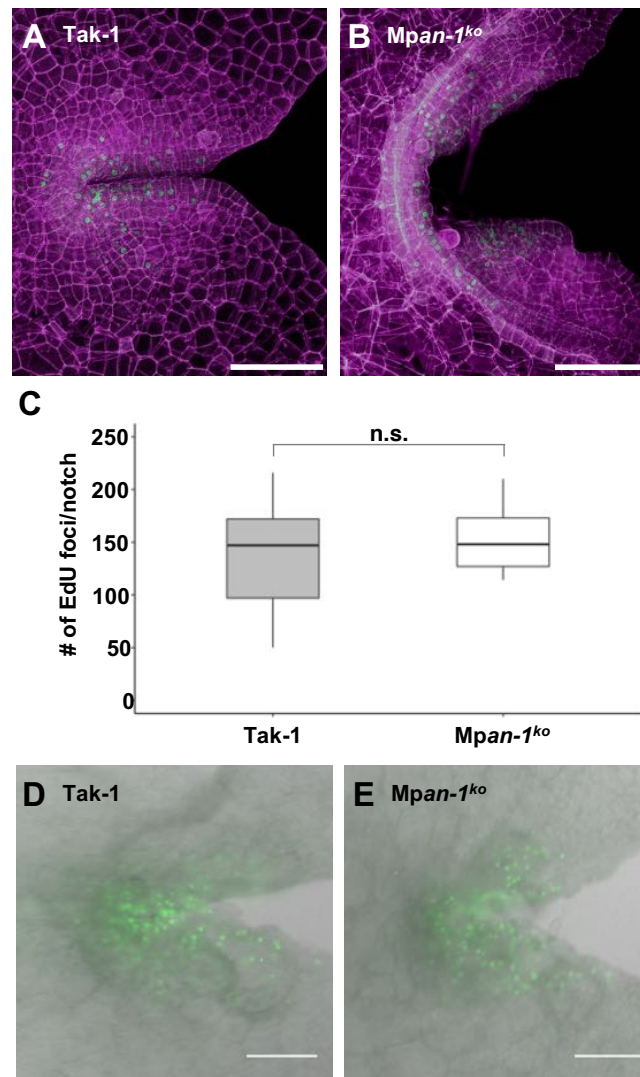




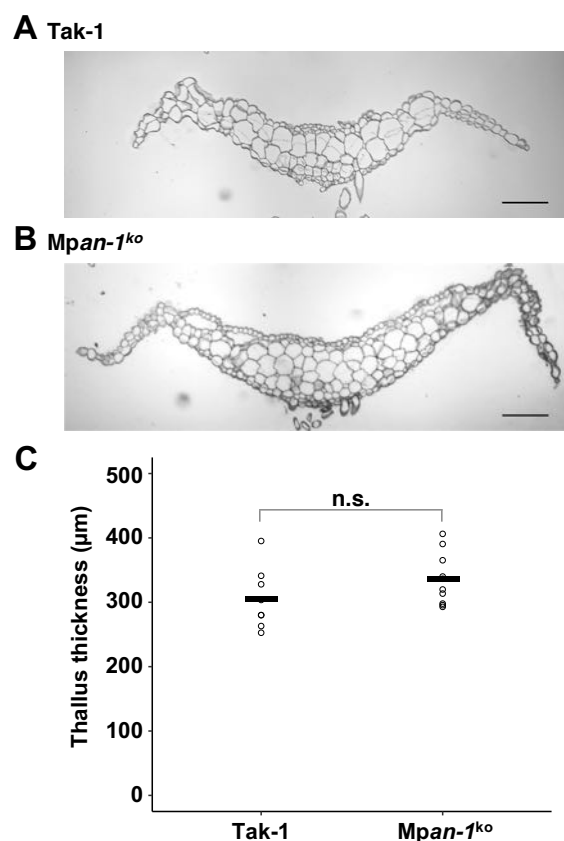
**Fig. S7. Shapes of the gemmae and thalli of *Mpan* mutants.** Shapes of the gemmae and thalli of Tak-1 and *Mpan-1<sup>ko</sup>* (male) cultured for 0, 1, or 3 days were visualized by mPS-PI staining. Cell walls stained with PI are shown in red. Bars, 200  $\mu$ m.



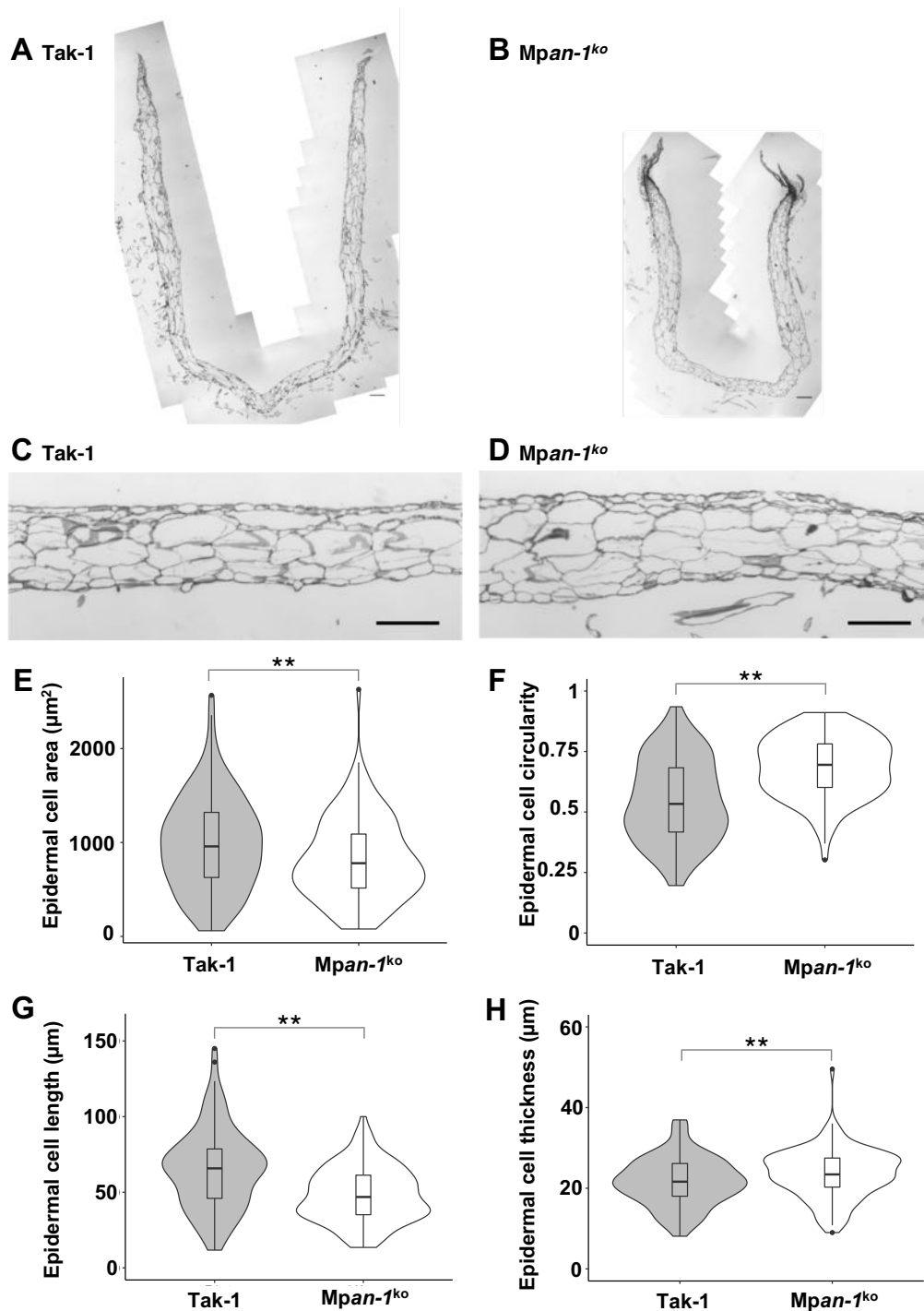
**Fig. S8. Thirty-five-day-old thalli of *Mpan* mutants.** (A, B) Tak-1 (A) and *Mpan-1<sup>ko</sup>* (male) (B) were cultured on rockwool for 35 days. Bars, 1 cm.



**Fig. S9. Numbers of S-phase cells in *Mpan* mutants.** (A, B) S-phase nuclei and cell walls in the Tak-1 and *Mpan-1<sup>ko</sup>* (male) lines cultured for 3 days were visualized by EdU and mPS-PI staining, respectively. Plants were treated with EdU-containing liquid medium for 1 h. Z-series fluorescence images were obtained. Maximum projection images of Tak-1 (A) and *Mpan-1<sup>ko</sup>* (male) (B) are shown. EdU-containing nuclei are shown in green and PI-stained cell walls in red. Bars, 100  $\mu$ m. (C) The numbers of EdU-containing nuclei are shown in box-and-whisker plots. Number of notches,  $n = 13$  (Tak-1) and  $n = 15$  (*Mpan-1<sup>ko</sup>* (male)). Asterisks indicate significant differences from Tak-1 (\* $P < 0.05$ , \*\* $P < 0.01$ , Student's  $t$ -test). (D, E) S-phase nuclei in the Tak-1 and *Mpan-1<sup>ko</sup>* (male) lines cultured for 5 days under weak blue light were visualized by EdU staining. Plants were treated with the EdU-containing liquid medium for 2 h. EdU-containing nuclei are shown in green overlaid with bright field image. Bars, 100  $\mu$ m.

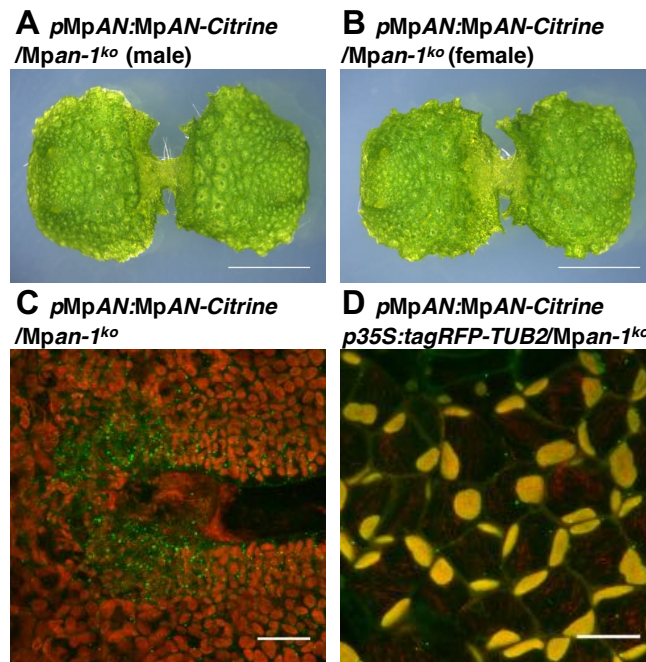


**Fig. S10. Thickness of thalli in *Mpan* mutants under weak blue light.** (A, B) Whole images of the transverse section of Tak-1 (A) and *Mpan-1<sup>ko</sup>* (male) (B) cultured for 10 days under weak blue light. Bars, 200 μm (A, B). (C) Thicknesses of thalli are shown in violin plots. Black dots indicate values of each measurement. Black bars indicate means of thickness values.  $n = 4$  (Tak-1) and  $n = 5$  (*Mpan-1<sup>ko</sup>* (male)). Significant differences compared with Tak-1 (\*  $P < 0.05$ , \*\*  $P < 0.01$ , Student's  $t$ -test).

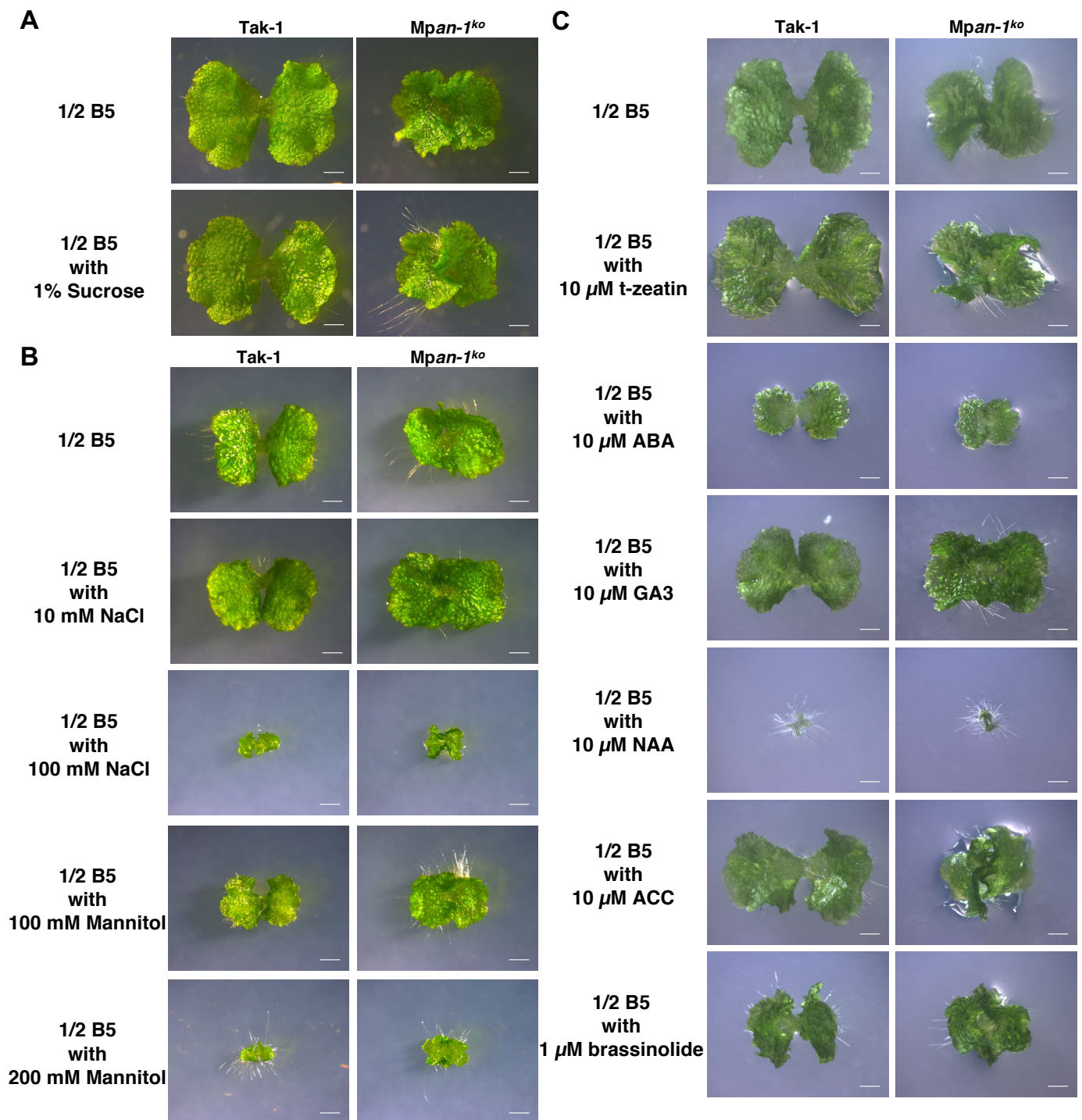


**Fig. S11. Epidermal cell Morphology in *Mpan* mutants under weak blue light.** (A, B, C, D) Whole images (A, B) and magnified images (C, D) of the longitudinal section of Tak-1 (A, C) and *Mpan-1<sup>ko</sup>* (male) (B, D) cultured for 10 days under weak blue light. Bars, 200  $\mu\text{m}$  (A, B, C, D). (E, F, G, H) Epidermal cell area (E), circularity (F), length (G), and thickness (H) are shown in violin plots with box-and-whisker plots. 108 cells from four individuals for Tak-1, and 123 cells from three individuals for *Mpan-1<sup>ko</sup>* were examined. Asterisks indicate significant differences compared with Tak-1 (\*  $P < 0.05$ , \*\*  $P < 0.01$ , Student's  $t$ -test).

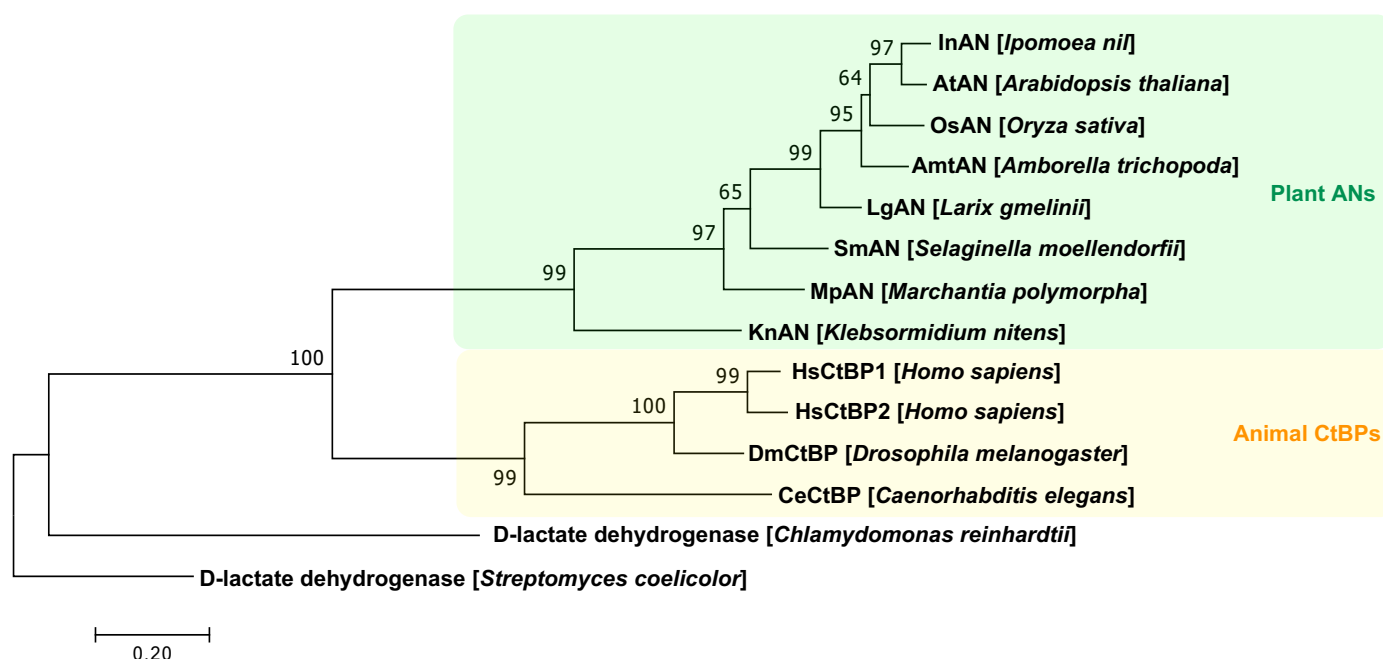




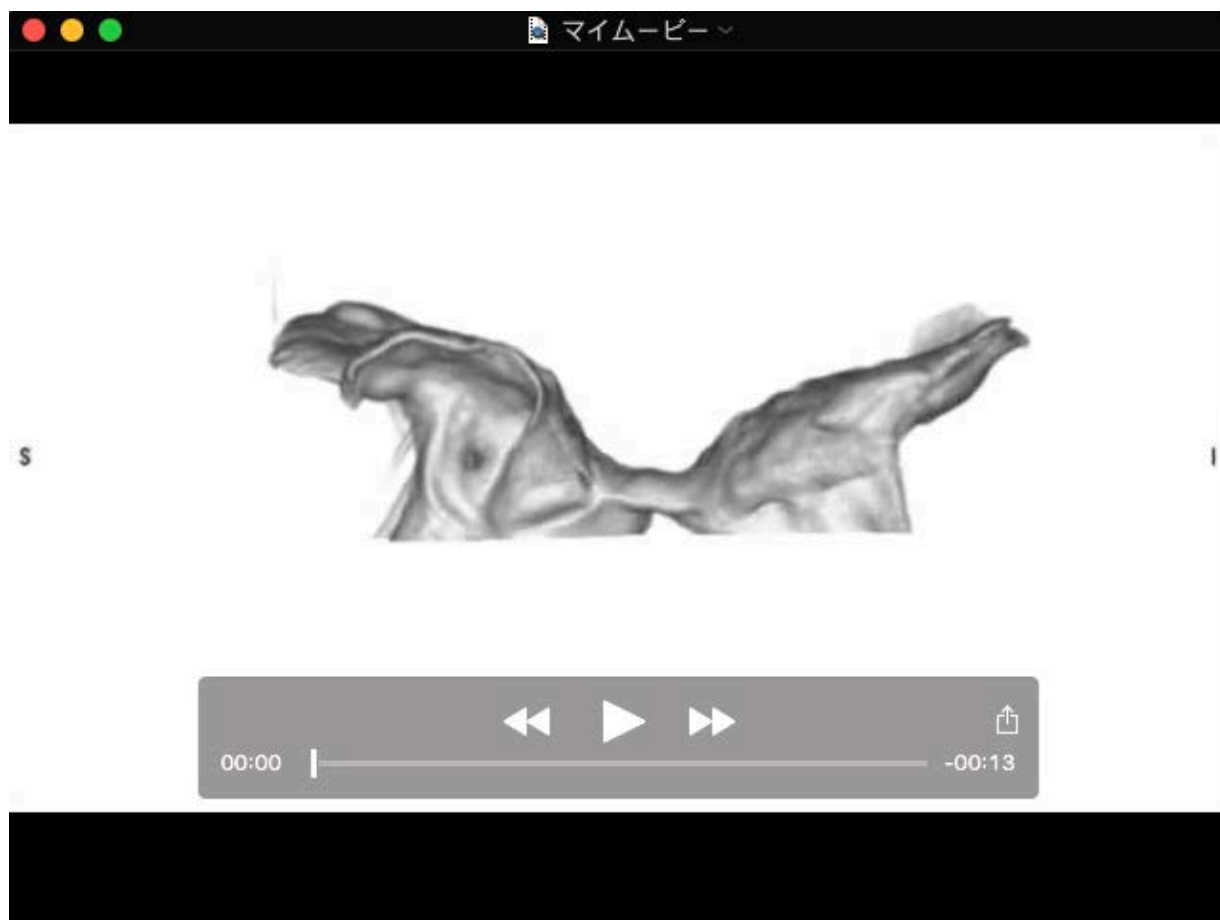
**Fig. S12. Subcellular localization of MpAN-Citrine protein.** (A, B) 10-day-old gemmalings of *pMpAN:MpAN-Citrine/Mpan-1<sup>ko</sup>* (male) (A) and *pMpAN:MpAN-Citrine/Mpan-1<sup>ko</sup>* (female) (B). Bars, 3 mm. (C) Subcellular localization of MpAN:Citrine in 2-day-old gemmalings of *pMpAN:MpAN-Citrine/Mpan-1<sup>ko</sup>* (male) transgenic plant was visualized. Citrine signals are shown in green and autofluorescence in red. (D) Subcellular localization of MpAN:Citrine and TagRFP-TUB2 in thallus of the *pMpAN:MpAN-Citrine/pCaMV35S:TagRFP-MpTUB2/Mpan-1<sup>ko</sup>* (male) transgenic plants was visualized. Citrine signals are shown in green, TagRFP signals in red and autofluorescence in yellow. Bars, 20  $\mu$ m (C, D).



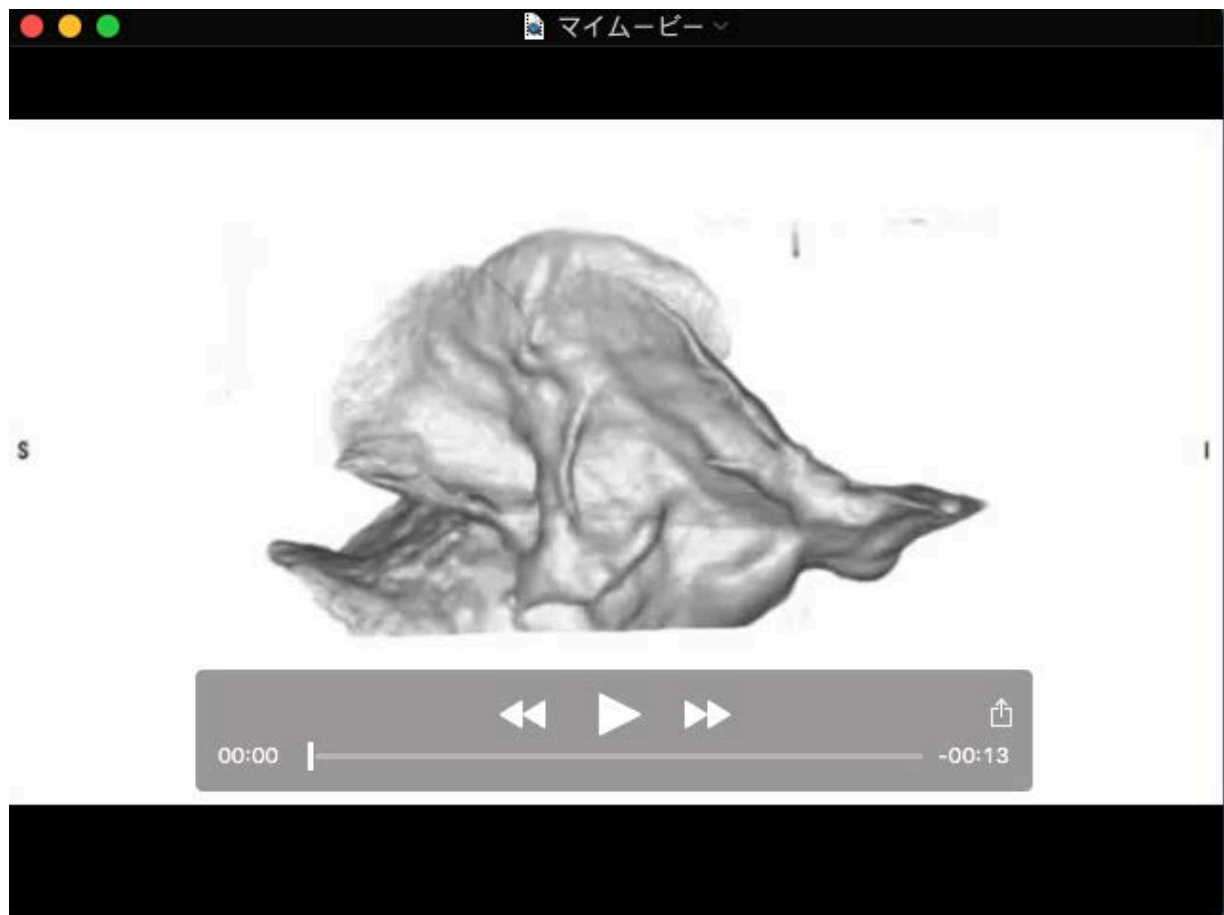
**Fig. S13. Morphology of *Mpan* mutants cultured on various environmental condition and phytohormone treatments.** Tak-1 and *Mpan-1<sup>ko</sup>* were cultured for 10 days on each indicated culture medium to test the response to sucrose (A), salt and osmotic stresses (B), and phytohormones (C). Bars, 1 cm.



**Fig. S14. Phylogenic analysis of plant ANs and animal CtBPs.** Phylogenetic analysis of the amino acid sequences of plant ANs and animal CtBPs was carried out. D-lactate dehydrogenases of *C. reinhardtii* and *Streptomyces coelicolor* were evaluated. The amino acid sequences of the D2-HDH motifs were aligned using CLUSTALW, and a phylogenetic tree was drawn using the maximum-likelihood method with bootstrapping of 1,000 replicates.



**Movie S1. Micro-CT image of a wild-type gemmaling.** Micro-CT image of a 10-day-old gemmaling of Tak-1.



**Movie S2. Micro-CT image of an *Mpan* knock-out mutant gemmaling.** Micro-CT image of a 10-day-old gemmaling of *Mpan*-*I*<sup>ko</sup> (male).